ASME GT 2015-42251

GOAL DRIVEN SHAPE OPTIMISATION FOR CONJUGATE HEAT TRANSFER IN AN EFFUSION COOLING PLATE

W. Savastano[3], A. Pranzitelli[4], G. E. Andrews[1], M. E. Biancolini[3], D. B. Ingham[2], M. Pourkashanian[2]

[1]Energy Research Institute; School of Chemical and Process Engineering, University of Leeds, UK; [2]ETII, University of Leeds, UK, [4]ANSYS UK Ltd, Sheffield, UK and [3]Università degli studi di Roma Tor Vergata
Email: savastano.walter@gmail.com or profgeandrews@hotmail.com

ABSTRACT

Full coverage effusion cooling was numerically investigated by means of conjugate heat transfer (CHT) computational fluid dynamics (CFD) for an array of effusion cooling holes in order to maximise the overall cooling effectiveness for a fixed coolant mass flow rate G, kg/sm^2. The baseline case study consisted of a 152x152x6.35mm perforated wall with a 300 K, 0.18 kg/sm^2 coolant flow through a square array of 90° effusion holes. The plate was mounted in a 770 K duct crossflow. The numerical model was validated against the experimental work of Andrews et al. (1990) and showed a maximum disagreement between the prediction and the experimental data of 3%. The effects of three geometrical parameters, i.e. the inclination of the holes, the pitch in X direction and the pitch in Y direction, on the overall cooling effectiveness were investigated without varying the coolant flow rate. The inclination of the effusion holes was varied between -33° and +33° from the plane of the plate, while the pitch in both directions was varied between 10.64mm and 19.76mm. The numerical investigation was performed using the commercial software ANSYS Workbench following a design of experiments approach. The geometrical modifications were obtained automatically in the CFD solver ANSYS Fluent for each design point by means of the RBF Morph software. This avoided the manual modification of the geometry and the subsequent mesh generation. The optimised configuration was obtained considering the maximisation of the average overall cooling effectiveness as a goal and a chosen minimum value for the local cooling effectiveness of 0.4 as the constraint. The results showed that the inclination of the effusion holes and the pitch in the Y direction have a greater impact on the cooling effectiveness than the pitch in the X direction, up to 17%, 28% and 5% from the baseline, respectively, within the range of values considered. An optimal combination of the three parameters was determined.

INTRODUCTION

One of the major means of achieving high performance turbines has been to increase the thermal efficiency of the engine using higher turbine entry temperatures. Better cooling techniques are required to maintain the combustor and turbine blade metal walls at acceptable temperatures. Film cooling is an effective method for turbine blade and nozzle wall cooling, but the air flow required for this lessens the thermal efficiency, as all of the compressor work on this air is not recovered in the turbine expansion. The minimisation of the proportion of the mass of compressor air used for film cooling is one of the challenges for future gas turbine engine design. The present work is focused on effusion cooling designs that enable the coolant mass flow to be minimised and was carried out with gas turbine combustor cooling as the design objective.

For combustors a plenum chamber air feed to effusion cooling holes is common and this was the basis of previous work on effusion cooling by Andrews and co-workers [14-17]. They extensively investigated experimentally the effusion film cooling on a conjugate heat transfer basis for practical gas turbine geometrical configurations. Their experimental designs were for combustor liner effusion cooling, but their results have relevance to turbine blade cooling. They measured the temperature of the crossflow gas in the effusion film cooling boundary layer at a point close to the wall to deduce a pseudo adiabatic film cooling effectiveness, as well as measuring the overall cooling effectiveness. All of their work was carried out with a plenum duct feed of the effusion air, which is a common combustor wall cooling air supply method in industrial gas turbines.

Improved fuel economy, specific power and lower NOx emission levels has been the main driving force for the continuing demand for high performance gas turbines. Primarily, a high performance gas turbine is achieved by increasing the thermal efficiency of the engine. However, this is somewhat a conflicting goal as the increasing thermal efficiency requires increased turbine entry temperatures (TET) which usually generate higher NOx emissions and generally

requires more wall cooling air mass flow. This additional wall cooling air is taken from the combustor airflow and this increases NOx, as the combustor primary zone operates hotter [2].The literature on film cooling of gas turbines is focused on single rows of film cooling holes, while effusion cooling has received relatively less attention. Effusion cooling combines good film cooling with good internal wall heat transfer and has the potential for high cooling performance with reduced cooling air mass flow. Effusion cooling has applications for turbine blade cooling and for low NOx combustor wall cooling [2].

There are two ways of reducing the coolant mass flow rate: improving the effectiveness of film cooling and improving the effectiveness of the overall cooling, which relates to the hole array design and the internal wall cooling. Inclined cylindrical hole injection was introduced to reduce the jet momentum normal to the cooled wall surface, as a means of improving the film cooling performance [3, 4]. The majority of these studies on film cooling utilise 30° or 35° injection angles. The poor transverse spread of the jet was the main weakness and this was the principle reason for the poor surface average film cooling performance of inclined film cooling holes.

Andrews and co-workers [5, 6, 7, and 8] have investigated experimentally the conjugate heat transfer in metal effusion walls. This is directly related to heat transfer in round holes, where the thermal development in the pipe entry regions dominates short hole heat transfer. Hot wall measurement techniques were shown to give good agreement with classic short hole heat transfer data. A further component of the heat transfer in the effusion wall is the acceleration of the coolant flow across the surface of the wall as it enters the hole.

One of the earliest experimental studies of effusion cooling on a conjugate heat transfer basis was reported by Esgar [9]. He found that, for the hot gas and coolant air supply temperatures of 1800 K and 811 K, respectively, the temperature rise of the coolant jet at the exit of the hole was about 250 K. Thus the exiting jet temperature would be 1061 K and the density ratio would be reduced from 2.2 to 1.7. Conjugate heat transfer experimental measurements for effusion cooling are rare and the only work similar to that of Andrews and co-workers [10, 11] is that of Kasagi [12] and Kumada et al. [13].

Yavuzkurt et al. [18] measured the turbulence and velocity profiles over an effusion film cooling flat plate. They found that the turbulence kinetic energy level within the boundary layer decreases with an increase in blowing ratio (M) due to the low velocity gradients at high M. The flow field of effusion film cooling jets was investigated by Scrittore et al. [19]. They demonstrated that sparsely spaced effusion cooling holes had a unique scalable velocity profile.

Harrington et al. [20] investigated the effects of the mainstream turbulence on the effusion film cooling performance. Short normal injection holes, similar to those employed by Andrews and co-workers [21-23], were used in their studies. They found that high mainstream turbulence reduced the film cooling performance more at low blowing ratios than at high blowing ratios with jet lift-off. The present predictions were for a high turbulence in the crossflow, created by a grid plate upstream of the test section.

Jeromin et al. [24] calculated the heat transfer coefficient of an effusion wall with a staggered hole array. The numerical results of their heat transfer coefficients demonstrated a good match with the experimental data for low blowing ratios. The present work did not investigate square and staggered hole arrays, but did investigate the transverse pitch Y of the holes for a fixed axial pitch X.

The need to accurately quantify cooling performance of real metal blades and combustor walls has led to the renewed interest in conjugate heat transfer studies by several gas turbine film cooling workers [25-29]. However, to our knowledge, there have been no previous conjugate heat transfer predictions of experimental hot wall data that separates the adiabatic film cooling from the overall cooling effectiveness and used CFD for the optimization of the design.

Simulation driven design is growing as an effective approach toward complex industrial and research applications. A very well established calculation workflow consists in the set-up of a high fidelity Computational Fluid Dynamics (CFD) model that has first to be validated against experiment results with convergence checks. Such a baseline model can then become parametric with respect to shape using mesh morphing. It can then be used to drive the optimization of the design using advanced computational tools. For the latter task metamodelling, i.e. evaluation of system response using a Design of Experiment (DOE) table interpolation to chase optimal configurations, is nowadays a standard practice.

Parameterization of the shape is one of the most delicate things to tackle and mesh morphing is emerging as a meaningful approach to have parametric shape directly at the CFD model level. New shapes are generated by deforming the mesh of the baseline CFD model, i.e. just updating nodal positions, which requires a negligible computational time compared to any remeshing procedure. Importantly, preserving the same mesh structure eliminates the remeshing noise that can be confused with the effect of the design parameters.

Several algorithms have been explored for this task. A common and well-established technique, the Free Form Deformation (FFD) [30] method, deforms volumes and controls their shape using a trivariate Bernstein polynomial. The method is meshless, so it can be easily implemented in parallel partitioned meshes with hybrid elements.

It allows the definition of new interesting shapes but it lacks accurate local surface control. Such accurate control can be achieved using mesh-based methods, for example in the pseudo solid method [31], where an elastic FEM solution is used to propagate the deformation inside. Parallel implementations can in this case be difficult and extra effort is required when surface movements are not known in advance. The meeting point between these two approaches can be achieved using Radial Basis Functions (RBF) interpolation that combines the benefits of a meshless method with great precision. In this case the RBF morphing field is interpolated using a cloud of points with given displacements. Even if there is interesting research demonstrating that RBF can be successfully adopted for the deformation of CFD meshes [32, 33], their numerical cost has limited their application in the past (direct solution grows by N3 where N is the number of RBF centres). The first industrial implementation of RBF mesh morphing was introduced in 2009

with the software RBF Morph [34] that comes with a fast RBF solver for the bi-harmonic kernel whose performance scales as $N^{1.6}$. A complete description of the tool is given in [35] while examples of applications can be found in Caridi and Wade [36], Cella and Biancolini [37], Khondge and Sovani [38] and Biancolini et. Al [39].

The aforementioned numerical approach is explored in the present study with the aims to validate conjugate heat transfer effusion cooling predictions, so that the procedures are applicable to any engine configuration. The CFD procedures are validated against experimental data and include the modelling of a gas tracer to simultaneously separate the surface distribution of the adiabatic film cooling from the overall cooling effectiveness, which could not be measured on the experimental test rig.

The validated numerical model is then parameterized with respect to its shape so that pitch can be continuously varied both in the X and Y directions; an offset in the inclination of the holes (identical for all ones) is introduced as the third design parameter. A fully automated workflow permits evaluation of the effect of shape on the synthetic performances of the system represented by the average overall effectiveness, the average adiabatic effectiveness, the maximum overall effectiveness and the maximum adiabatic effectiveness.

GEOMETRY INVESTIGATED:

This study investigated the geometry presented in [1]. Full coverage effusion cooling was studied for a square array of 90° effusion cooling holes with a plenum chamber air supply to the coolant holes. Active cooling was used with metal walls and 300 K effusion cooling into a 27 m/s mean velocity duct flow at 770 K crossflow temperature. The 152 mm square test section had 10 rows of holes with hole diameter, D = 3.27, and hole pitch X=15.2. The X/D value studied was 4.6. At a constant coolant mass flow rate the wall pressure loss was reduced as X/D was reduced and there was an associated reduction in the film blowing ratio, M. The duct air feed to the holes enhanced the backside cooling of the wall. Several walls were tested in [1], with different ratio X/D; hole pitch X was also varied for a constant hole diameter D, and vice versa. Decreasing X/D was the most effective way of increasing the overall cooling effectiveness, as this reduced the blowing rate without decreasing the coolant mass flow rate. This was more effective than using 30° inclined holes with an X/D = 11, as the hole exit velocity was much lower for the same coolant mass flow rate with 90° holes at an X/D = 4.6. The experimental apparatus of Andrews et al. (1990) [1] is shown in Fig.1.

The effusion wall designs investigated in this study consist of a square array of normal injection holes with an exposed squared surface area of 152 x 152 mm. The injection hole length, L, was 6.35mm for all the wall designs. The key design variable investigated had a 10×10 square array of holes with a total number of holes per square metre surface area, N=4306 holes/m^2, as shown in Fig.2. Because of the symmetry of the apparatus only a slice of it was used in the simulations, giving symmetry condition to the side boundary as in Fig.3.
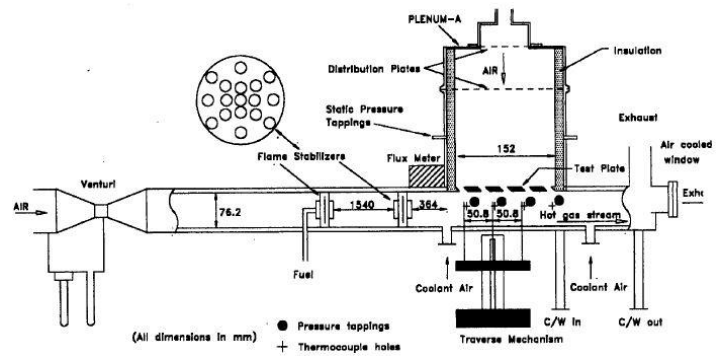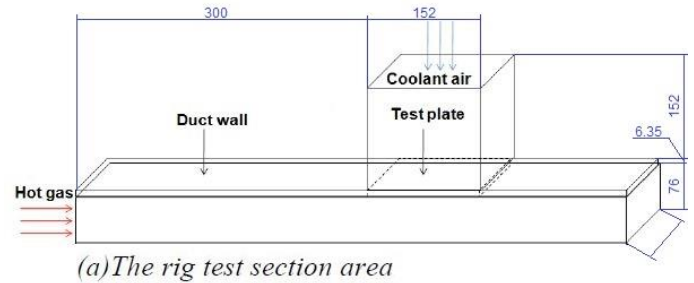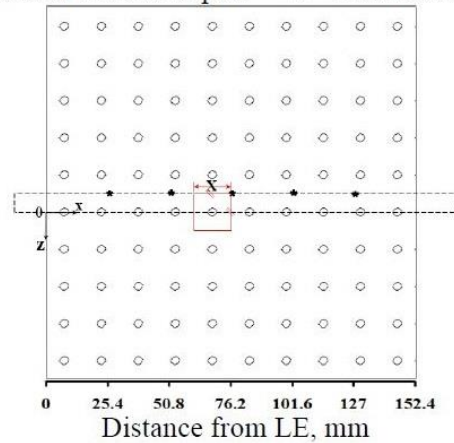

Fig1. Experimental apparatus

(a)The rig test section area

* - Embedded thermocouples   o - Film cooling holes

(b)Wall E with the 10×10 square array of holes, thermocouple arrangements and computational domain
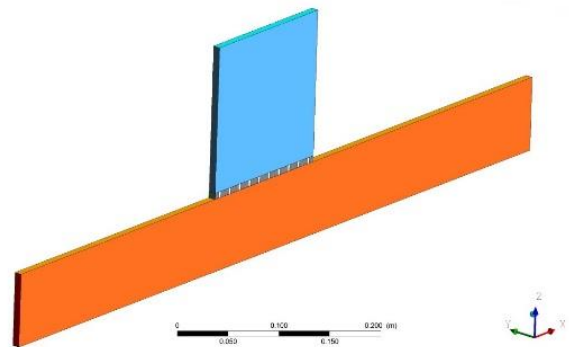
Fig.2 Schematic of the rig test area

Fig.3 Computational geometry

EXPERIMENTAL PROCEDURES

The overall effectiveness η_{ov} is given by equation 1:

$$\eta_{ov} = \frac{T_g - T_w}{T_g - T_c} \qquad 1$$

where T_g is the temperature of the hot gas, T_c is the temperature of the cooling air, T_w is the measured metal temperature from the imbedded thermocouples shown in Fig.2. These were located on the centreline between the effusion holes and thus were at the hottest part of the metal wall. This was done so that the measured cooling effectiveness data would be conservative. The hottest part of the metal wall would be the part to fail first and hence the determination of the hottest wall temperature was important in the experimental work. The experimental uncertainty in the determination of η_{ov} was mainly due to the measurement of T_g, as T_c was close to ambient temperature and the metal temperature T_w was steady.

The test wall was mounted in an air cooled duct that contained the hot crossflow, heated by an 2m upstream natural gas directly fired air heater. The has gas crossflow passed through two grid plates before the test section so that a uniform temperature and velocity was achieved. The test wall was mounted 300mm downstream, of the final grid plate which had a 3% pressure loss which was typical of gas turbine combustors and generated typical levels of crossflow turbulence. A 10% crossflow turbulence was assumed in the computations. The air cooled duct had an adjustable air cooling flow rate that was adjusted to keep the duct wall at the same temperature as the middle of the test wall. This avoided radiation interchange between the test wall and the duct.

The hot gas temperature was measured by a bare bead thermocouple mounted 50 mm away from the centre of the test wall. There was no correction made for radiation losses, and it was considered that at the 27 m/s crossflow velocity the convective gain was high and the radiative loss was low, as none of the walls were water cooled. However, the error was significant, but it was considered that a suction pyrometer would be too bulky and the gas suction would interfere with the duct aerodynamics. The overall effectiveness equation is a ratio involving the temperature difference from the gas temperature, and the error was largely cancelled out. However, T_g would always be low due to the radiant heat losses to the cooler walls.

Calculations of the worst case heat losses and the convection heat gain from the hot crossflow using a cylinder in a crossflow heat transfer, give the maximum T_g error of 20 deg. This gives a maximum underestimation of η_{ov} of 0.02 at the highest coolant flow rate, which gives the highest temperature difference. This is about a 4% cooling effectiveness error for the baseline cooling effectiveness of 0.5.

The experimental flat effusion walls that were modelled were made from Nimonic-75. The experimental test rigs consisted of an insulated coolant air plenum chamber mounted in the top wall of the 76-mm-deep by 152.4-mm-wide duct. The test plates, with an array of equispaced lateral and streamwise hole pitch, X, formed the bottom part of the plenum chamber which was bolted to the plenum chamber. The plenum chamber was insulated internally to prevent heat loss from the coolant to the plenum wall.

Surface averaged overall cooling effectiveness was not directly measured, but it was assumed that internal wall conduction would effectively locally average the heat transfer. This occurs at low Biot numbers which was the case in the experimental work. The choice of the worst case location in the experiments for the measuring thermocouple was to ensure that the resultant overall cooling effectiveness was conservative, as the results were to be directly applied in gas turbine combustor design. The thermocouples were located at 25.4, 51.8, 76.2, 101.6 and 127 mm from the leading edge. These locations were kept fixed for all the experimental test walls, so that comparison could be made for effusion cooling where N was a variable while the length of metal to be cooled was fixed. This enables comparison between different designs at the same axial location from the leading edge.

COMPUTATIONAL PROCEDURES

The computational domain was discretised with a multiblock structured mesh generated with ANSYS ICEM CFD software. All the walls of the computational domain, except for the metal plate were modelled as adiabatic. A mass flow inlet boundary condition was used at the coolant inlet with a mass flow rate of 0.18kg/sm2 and a temperature of 300K. The hot cross flow inlet was modelled as a velocity inlet with a flow velocity of 27m/s and T=770K, corresponding to the experimental conditions. The outlet was modelled as a pressure outlet with atmospheric pressure. The turbulent intensity at the inlets was assumed 5%, although no experimental data are available.

The Reynolds number referred to the hydraulic diameter in the hot crossflow is about 27000 while it varies from 1000 to 3000 in the holes, depending on the hole. For simplicity the flow was considered fully turbulent, also because the exit region of the holes is turbulent. A realizable k -ε turbulence model was employed when assessing the sensitivity of the results to the computational mesh, since it was already employed in previous film cooling studies successfully [40-44]. A coarse mesh, made of about 600k cells, was refined in the near wall region of the plate to obtain a medium mesh of about 900k cells. To assess the grid independency of the results, the medium mesh was further refined in the plate region including the inlets and outlets of the holes. The cells affected by the refinement were split in the three directions. The fine mesh consisted of 4.3m cells. The enhanced wall treatment was used to model the flow field near the solid walls of the domain.

The flow condition used for the baseline predictions with experiments was a coolant flow of 0.18 kg/sm^{2}bar, which is a blowing ratio, M, of 0.4. This represents about 10 % of the total combustor air flow used for film cooling, which is much lower than current effusion cooling air mass flow usage. The overall cooling effectiveness is low for the baseline, as shown in Figs. 4 and 5, with a trailing edge overall cooling effectiveness of 0.55 compared with a desired cooling effectiveness for wall survival of 0.7. The objective was to investigate the improvement in this poor performance with 90° effusion holes that could be achieved by optimization of the hole design using CFD.
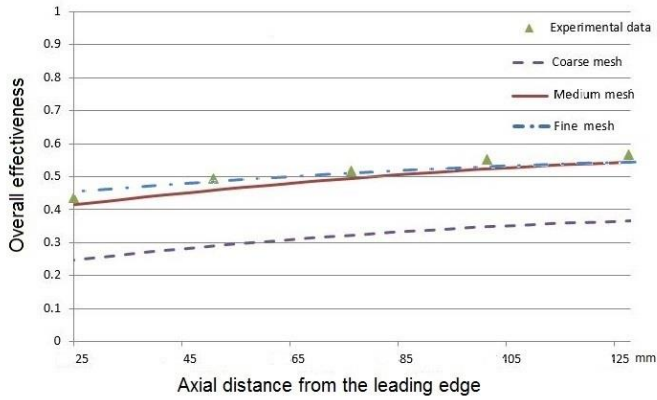
Fig.4 Overall effectiveness along the centerline as a function of distance from the leading edge for the coarse and refined mesh for10 rows of 90° effusion holes with an X/D of 4.6 and N = 4306/m² for a coolant mass flow rate G of 0.18 kg/sm²bar or M of 0.4.
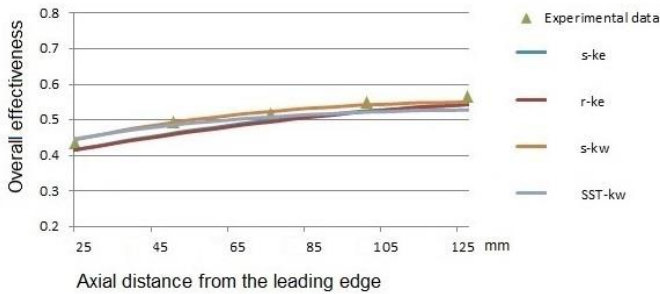

Fig.5 Influence of the CFD turbulence model on the prediction of the overall cooling effectiveness with comparison with the experimental data, for G= 0.18 kg/sm².

The resultant predicted overall effectiveness was compared with the experimental results in Fig.4 for the above coarse, medium and fine meshes. This shows that the medium mesh provides a reasonable agreement with the experimental data, with small differences with the fine mesh, therefore it was used for the rest of this study. The predictions in Fig. 4 obtained by means of the medium mesh were slightly low by about 4%, which is the same as the measurement error and hence is not significant.

The influence of the turbulence model on the overall cooling effectiveness was investigated by comparing the baseline computation that used the realizable k-ε model and comparing it with the standard k –ε , the k-ω and the SST k-ω turbulence models. This comparison is shown in Fig. 5 which shows that the influence of the turbulence model was relatively small. It should be noted that the turbulence model influences the heat transfer in the effusion wall as well as in the film cooling boundary layer. In both cases flow separation and reattachment occurs. This occurs inside the hole for the wall cooling and as a lifted jet in the film cooling boundary layer. The realizable k-ε model copes with flow separation and reattached flows well, which is why it is appropriate in the present work. Fig. 5 shows that in the present work all the turbulence models gave good agreement with the experiments, to within the +/-4% accuracy
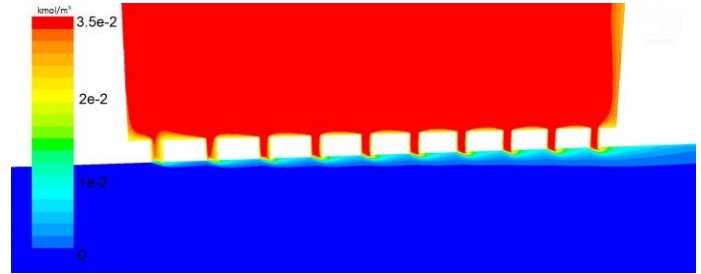

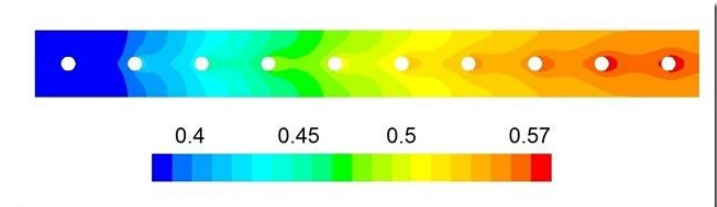Fig.6 Scalar coolant tracer profile on symmetry plane.

Fig.7 Overall cooling effectiveness distribution on the wall for G – 0.18 kg/sm²bar

of the experimental measurements of cooling effectiveness. The maximum difference between the four turbulence models was 4% in cooling effectiveness. The realisable k- ε was used in the rest of this study.

In these computations, as in the work of Ogentade et al. (40 – 44) a scalar tracer was added to the coolant so that its mixing with the crossflow (with zero tracer gas) could be predicted and visualised. The concentration of the tracer at the wall relative to the coolant concentration is the adiabatic cooling effectiveness in the presence of heat transfer in the wall. The visualization is most useful as it shows how well attached to the wall is the effusion cooling film. An illustration of this is shown in Fig. 6 for the 0.18 kg/sm²bar coolant flow (M = 0.4). This shows no penetration of the coolant jets into the cross flow, in spite of the 90° holes.

The crossflow smears the coolant along the surface and prouces a very thin coolant layer. The adiabatic cooling effectiveness is very low at this low coolant flow and most of the heat transfer occurs due to internal wall cooling. The peak adiabatic cooling effectiveness was 0.4 just downstream of the last rows of the ten holes. However, most of the wall was at an adiabatic cooling effectiveness of 0.15.This work concentrated on hole orientation changes that will improve the film cooling performance, or reduce the mixing of coolant and crossflow.

Fig. 7 shows the prediction of the baseline overall cooling effectiveness distribution over the effusion metal wall surface. Fig. 7 shows that the wall has a relatively low transverse profiles of cooling effectiveness. The colour contours in Fig. 7 are about 0.01 cooling effectiveness apart so that the maximum transverse gradient was predicted to be 0.02, which is very low. This was the assumption in the experimental work where thermocouples on the metal wall on the centerline between the hole, which is the edge position in Fig. 7, would measure the surface average cooling effectiveness. As the thermocouples were located at the hottest temperature region the experimental
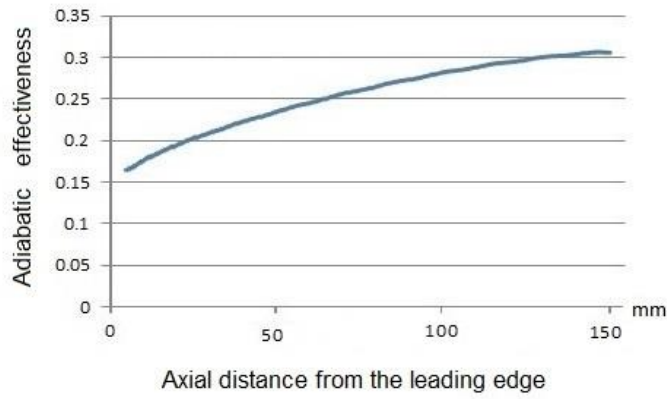
Fig.8 Pseudo adiabatic effectiveness along the centerline as a function of distance from the leading edge

results would be conservative. Fig. 7 shows that the axial gradient of the cooling effectiveness was significant, as also shown in Fig. 4.

The film temperature adjacent to the wall is the adiabatic temperature if there is no heat transfer to the wall. Its measurement in the present work with active heat transfer is referred to as a pseudo adiabatic cooling effectiveness.

$\eta_{ad}=(T_g-T_{w*})(T_g-T_c)$

The pseudo adiabatic wall cooling effectiveness was defined in the same way as for the overall cooling effectiveness, but uses the temperature of the gas adjacent to the wall at the midpoint of the square array of holes. This was a measurement of the worst case (furthest from the effusion jet centreline) heat transfer location. The pseudo adiabatic cooling effectiveness and its development with axial distance are shown in Fig. 8. Comparison with Fig. 6 shows a range of adiabatic cooling effectiveness on the hole centerline of 0.15 at the leading edge and 0.4 at the trailing edge. This is similar to the results in Fig. 8 but with higher trailing edge values. This is because the boundary layer has temperatures increased by the heat transfer in the wall, whereas the effect is not in the adiabatic cooling effectiveness computations in Fig. 6.

PARAMETERISATION

In order to optimize the geometry, three shape parameters were varied: the X-pitch and Y-pitch were changed independently so that the X/D and Y/D ratios were varied; the angle of injection was varied starting from 90 degree holes and including counter flow injection [22]. Fig. 9 summarises the chosen deformations, which were used as input parameters for the optimization process. This was done for a fixed effusion hole diameter. Future work will investigate the optimization of the hole diameter and shape.

The effusion wall design modifications were obtained by using the RBF Morph software directly within the CFD solver environment. The amplitude of the deformation was given by a base displacement multiplied by an adequate amplification factor. Table 1 shows the correspondence between amplification factors and deformations. Five output parameters were monitored for the optimization: the minimum, average and.
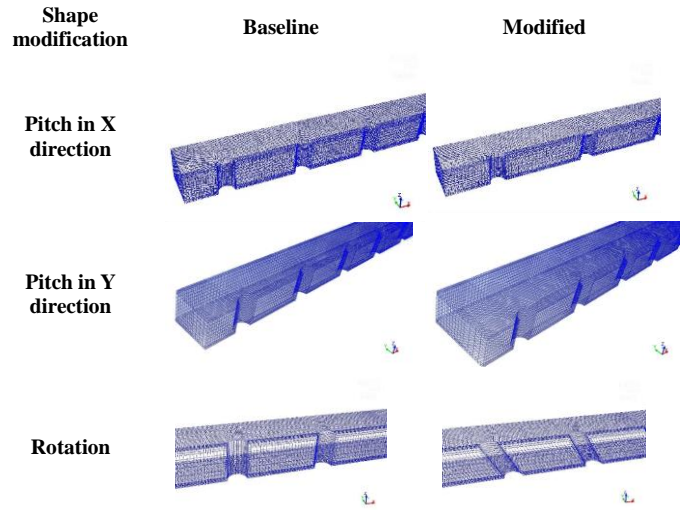

Fig. 9 Parameter and shape modification

	Rotation	Stretch X	Stretch Y
Amplification	Angle (deg)	Pitch-X (mm)	Pitch-Y (mm)
-6	/	10.64	/
-5	32.7	11.40	/
-4	39.0	12.16	/
-3	46.7	12.92	10.64
-2	57.8	13.68	12.16
-1	72.5	14.44	13.68
0	90.0	15.20	15.20
1	72.5	15.96	16.72
2	57.8	16.72	18.24
3	46.7	17.48	19.76
4	39.0	18.24	/
5	32.7	19.00	/
6	/	19.73	/

Table 1 Correspondence between amplification factors and actual shape variation

| Injection angle (deg)	Pitch in x (mm)	Pitch in Y (mm)	Over. Eff. Min	Over. Eff. Aver.	Over. Eff. max	Adiab. Eff. Av.	Adiab. Eff. Max
43°	18.8	19.5	0.408	0.468	0.616	0.243	0.356
90°	23.7	15.2	0.358	0.409	0.514	0.216	0.29
-51°	15.2	12.8	0.367	0.383	0.550	0.223	0.314
-43°	6.7	13.4	0.405	0.413	0.650	0.249	0.388
-78°	22.5	16.4	0.275	0.351	0.573	0.204	0.323
57°	10.3	18.8	0.369	0.416	0.548	0.220	0.310
-57°	21.3	11.6	0.284	0.351	0.557	0.210	0.319
-66°	17.6	17.6	0.424	0.445	0.643	0.258	0.382
-39°	7.9	17.0	0.381	0.389	0.576	0.228	0.319
51°	9.1	15.8	0.279	0.360	0.546	0.209	0.308
-35°	12.8	14.0	0.285	0.366	0.654	0.213	0.354
35°	11.6	10.9	0.338	0.407	0.596	0.242	0.342
66°	16.4	18.2	0.327	0.411	0.640	0.245	0.382
39°	14.0	14.6	0.393	0.480	0.563	0.232	0.315
78°	18.8	19.5	0.344	0.363	0.557	0.220	0.332

Table 2 Design of experiments table
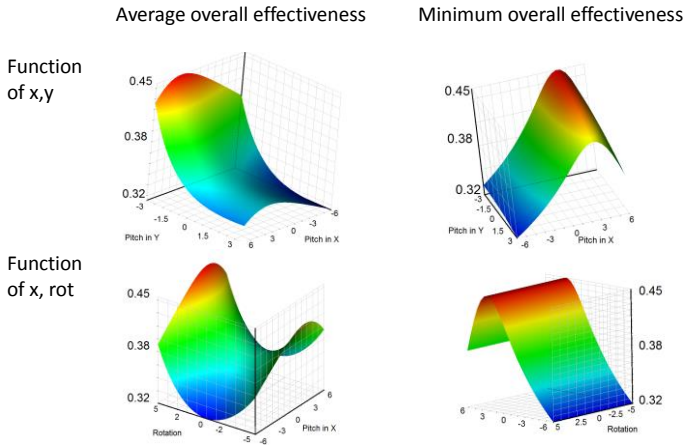
Fig.10 overall effectiveness minimum and average as a function of X,Y and X,Rot

maximum overall effectiveness, and the average and maximum adiabatic effectiveness

To investigate the effects of the geometrical parameters on the output parameters, a response surface metamodel was generated from a design of experiments table. The rotation of the hole axis was varied within ±32.7 degrees, while pitches in both directions were varied from 10.64 mm to 19.76 mm. The baseline conditions were 90° and 15.2mm.

Since the mesh is simply morphed by means of RBF Morph without any remeshing, the total number of cells remains the same during the geometric variations.

The design space was filled with 15 design points generated by using a Central Composite Design sample type and optimal space filling design of experiments type. Table 2 describes the design points with the corresponding output parameters obtained after CFD simulation. The CFD simulations were performed automatically within the ANSYS workbench environment. after the generation of the response surface, the search for the optimised configuration was performed considering the maximisation of the average overall cooling effectiveness as an objective function and a chosen minimum value for the local cooling effectiveness of 0.4 as the constraint. blowing ratio M is being reduced. This results in an increase in cooling effectiveness as shown in Fig.10. For an increase in X or Y from the baseline, the X/D and Y/D are being increased and at constant mass flow rate this increases the pressure loss and M. This will deteriorate the cooling effectiveness, but Fig. 10 shows this is a lesser effect than the increase in cooling effectiveness when Y is reduced.

The rotation of the hole axis in both directions increases the average overall effectiveness, but has negligible effect on the minimum overall effectiveness. The angle in the co-flow direction has the greatest improvement in the overall cooling effectiveness, but the opposed flow angle is quite effective [22].

RESULTS

The response surface allows the investigation of the effects of the geometrical parameters on the chosen output parameters. As can be seen from Figure 10, a reduction of the pitch in the Y direction leads to a significant increase of the average overall effectiveness, while the pitch in the X direction has minor effects on it. The pitch in the Y direction has, on the contrary, a minor effect on the minimum overall effectiveness, while a maximum value is obtained for a pitch in the X direction of about 17mm, close to the baseline condition.

Changing the pitch in the X or Y direction at constant hole diameter changes the X/D and Y/D and for values of either that are lower than the baseline X/D of 4.6 the number of holes is being increased and for the same mass flow rate the effusion wall pressure loss is being decreased, effectively the hole

N°	Injection Angle (deg)	Pitch in x (mm)	Pirch in Y (mm)	Over. Eff. Min	Over. Eff. Aver.	Over. Eff. Max	Adiab. Eff. Aver.	Adiab. Eff. Max
BASE	90	15.24	15.24	0.411	0.453	0.540	0.216	0.309
1	-32.7	17.03	12.92	0.483	0.591	0.681	0.316	0.392
2	-33.2	18.31	12.90	0.482	0.563	0.652	0.304	0.383
3	-74.6	16.72	12.90	0.524	0.603	0.668	0.338	0.403

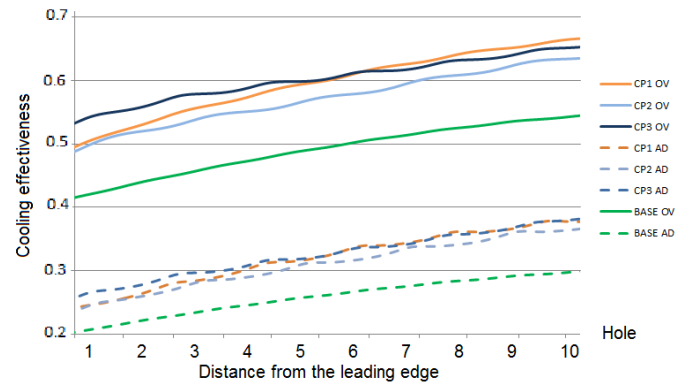Table 3 Candidate points as optimum, G = 0.18 kg/sm²bar and M = 0.4

Figure 11 Comparison of the effectiveness of the candidate points and the baseline geometry.

From the response surface metamodel, three optimum candidates were obtained, according to the objective function and the constraint chosen, as shown in Table 3 for a G of 0.18 kg/sm²bar. Table 3 shows that significant improvement can be obtained by modifying the geometrical parameter chosen. The same can be seen from Fig. 11, which shows the trend of average and minimum overall effectiveness in the X direction. Fig. 11 shows that the optimization process has identified geometries with significantly higher overall cooling effectiveness than the baseline. Candidate point 3 provides a flatter effectiveness curve than the other design points. This can be taken into account when high thermal gradients on the plate need to be avoided. It should be noted that all three optimum designs involve opposed flow effusion jets. These were first shown to be an effective direction for effusion jets outlets by Andrews et al. [22]. This work showed that above a critical G the opposed flow jets would lift off the surface and the cooling effectiveness would then deteriorate. For low G, as in the
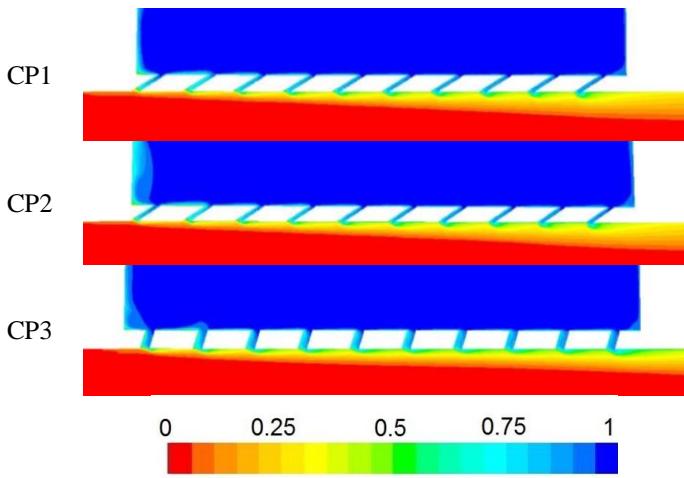
CP1

CP2

CP3

0   0.25   0.5   0.75   1

Fig.12 Overall dimensionless temperature profiles on the centreline of the effusion holes. $(T_g-T)/(T_g-T_c)$

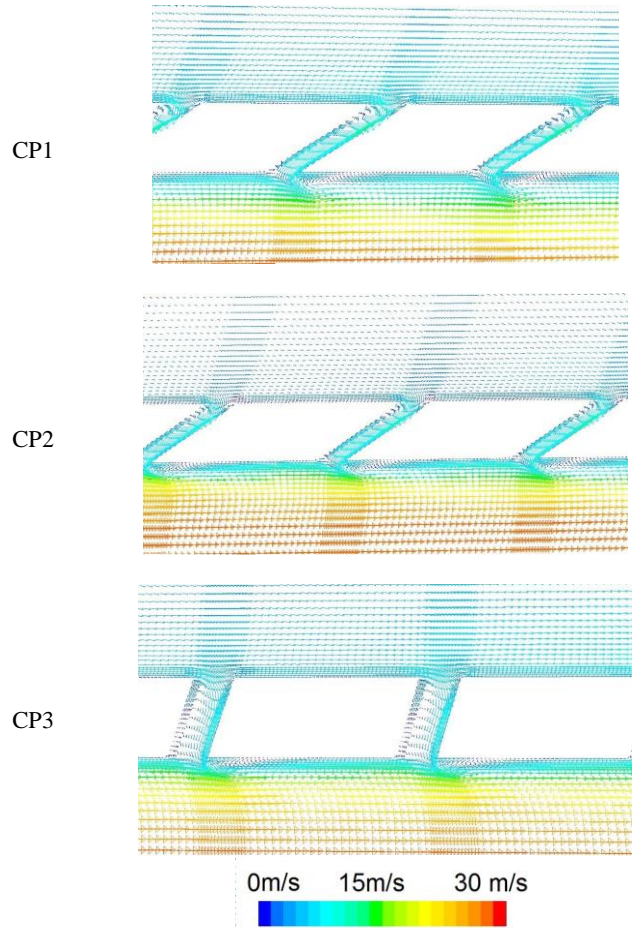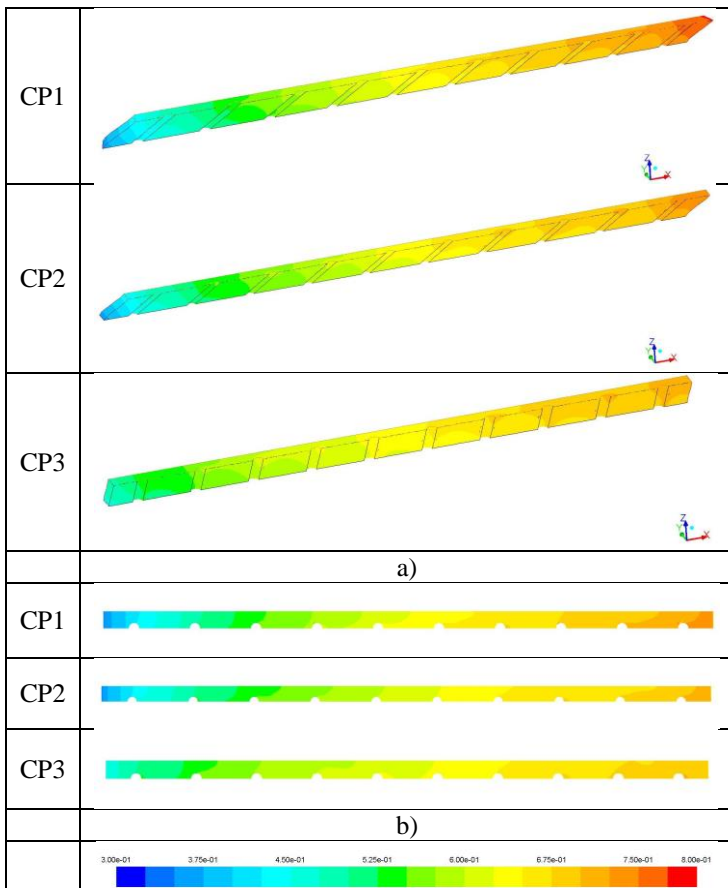|		
CP1		
CP2		
CP3		
	a)	
CP1		
CP2		
CP3		
	b)	
	3.00e-01 3.75e-01 4.50e-01 5.25e-01 6.00e-01 6.75e-01 7.50e-01 8.00e-01	

Fig. 13 Wall metal overall cooling effectiveness distribution a) and on the cooled surface of the plate b) for the three candidate points

CP1

CP2

CP3

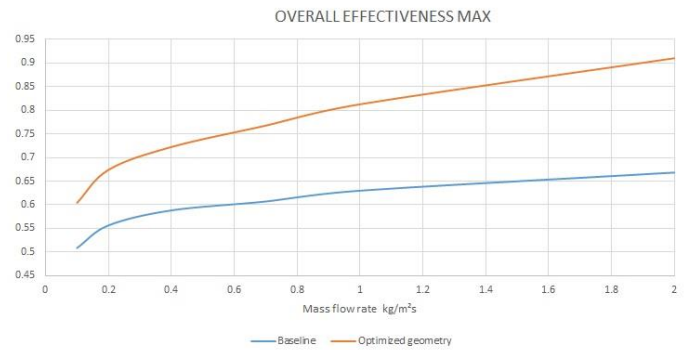0m/s   15m/s   30 m/s

Fig. 14 Velocity vectors on the symmetry plane

OVERALL EFFECTIVENESS MAX

Mass flow rate kg/m²s

— Baseline   — Optimized geometry

Fig.15 Maximum overall effectiveness of baseline and candidate point 3 as a function of G
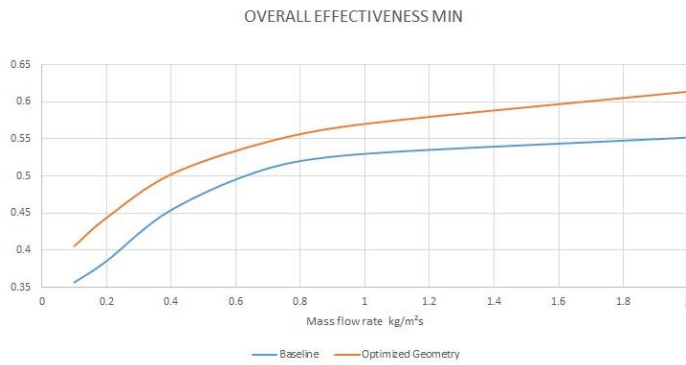
OVERALL EFFECTIVENESS MIN

Fig.16 Minimum overall effectiveness of baseline and candidate point 3 as a function of G

present computations the opposed jets have a reverse flow by the crossflow which forces the coolant film to spread across the surface much better than inclined jets in crossflow.

Figures 12-14 compare the results obtained by the three candidate points as dimensionless gas temperature, cooling effectiveness distribution through the metal thickness and on the cooled plate, and velocity vectors, respectively. Fig. 12 shows that all three geometries have no flow separation of the coolant jets from the surface and all the coolant flow remains attached to the surface.

Fig. 14 velocity profiles also show the flow remains attached to the wall. Fig. 14 also shows that the cooling inside the holes in the wall are enhanced by the flow separation at the hole inlet which with inclined holes keeps the high velocity flow along one wall and not in the centre of the hole. Fig. 15 shows that CP1 has the best cooling effectiveness distribution and Table 1 confirms that this is the best design.

Figs. 15 and 16 show the maximum and minimum overall effectiveness, respectively, as a function of the coolant mass flow rate G for the baseline and the candidate point 3, which gives the best effectiveness. It can be seen that the same effectiveness of the baseline geometry for a given flow rate can be obtained with the optimised geometry at a much lower flow rate. For instance, a maximum effectiveness of 0.6 can be obtained by using a coolant mass flow rate of 0.6 kg/sm^2 with the baseline geometry and 0.1 kg/sm^2 with the optimized geometry. Similar results can be obtained for the minimum overall effectiveness, as a value of 0.5 can be obtained with 0.62 and 0.4 kg/sm^2 with the baseline and the optimized geometry, respectively. Also, it is possible to see that a further increase of the coolant flow rate after a certain value does not provide significant improvement of the effectiveness.

CONCLUSIONS

Full coverage effusion cooling was numerically investigated by means of computational fluid dynamics (CFD) for an array of effusion cooling holes in order to optimise the overall cooling effectiveness.

The influence of hole density per unit surface area, and the influence of the injection angle, on the cooling performances, was investigated computationally using Fluent. Experimental data for validation was the hot rig metal wall effusion cooing data of Andrews et al. [1] at a coolant mass flow rate of 0.18

kg/sm^2 bar. The baseline geometry was an X/D of 4.6 and N=4306 holes/m^2 with 90° holes. This showed a maximum disagreement between the prediction and the experimental data of 3%.

The hole spacing in the axial and transverse directions were optimized together with the hole injection angle. The best overall cooling effectiveness distribution was for opposed flow effusion cooling jet injection at an angle of 32.7^o with an X/D of 5.2 and Y/D of 3.95 for a G of 0.18 kg/sm^2.

The optimised configuration was obtained considering the maximization of the average overall cooling effectiveness as a goal and a chosen minimum value for the local cooling effectiveness as a constraint. A design of experiment approach allowed the generation of response surfaces, i.e. surfaces that show the variation of the output parameters as a function of 2 input parameters for time, keeping the third input parameter constant. Results showed that the inclination of the effusion holes and the pitch in the Y direction had a greater impact on the cooling effectiveness than the pitch in the X direction, up to 17%, 28% and 5% from the baseline, respectively, within the range of values considered.

The optimisation procedure led to three candidate points, imposing the maximization of the average overall cooling effectiveness, and a minimum overall cooling effectiveness of 0.45. An optimal combination of the three parameters considered is finally proposed. Results showed that the new geometries produce improvements between 15-20% on the overall effectiveness, and 10% in adiabatic effectiveness. Furthermore, the third candidate point gives a lower thermal gradient, and therefore lower thermal stresses on the plate. Finally using the geometry proposed in the candidate point 3, an investigation on the influence of the coolant mass flow rate was undertaken. This showed that a given cooling effectiveness can be obtained with a much reduced coolant mass flow rate with respect to the baseline geometry.

Nomenclature	
η_{ov}	Overall cooling effectiveness
η_{ad}	Pseudo adiabatic cooling effectiveness
T_g	Temperature of the gas at hot inlet
T_c	Temperature of the air at the cold inlet
T_w	Temperature of the plate
T_{w*}	Temperature of the air at 0.2 mm from the plate, on the hot side.
X	Pitch in x direction
Y	Pitch in y direction
Rot	Rotation angle between the hole axis and the plate
G	Cooling mass flow rate
M	Blowing ratio
D	Holes diameter

REFERENCES

[1] G E Andrews, A A Asere, M L Gupta and M C Mkpadi, "Effusion cooling: the influence of the number of holes"

Proceedings of the Institution of Mechanical Engineers, Part A: Journal of Power and Energy 1990 204: 175

[2] Andrews, G. E. and Kim, M. N., 2001, "The influence of film cooling on emissions for a low radial swirler gas turbine combustor,"
Proc. ASME International Gas Turbine & Aeroengine Congress & Exhibition, New Orleans, ASME Paper GT2001--GT--71.

[3] Goldstein, R.J., 1971, "Film Cooling. Advances in Heat Transfer", Vol. 7 pp. 321-379.

[4]Crawford, M.E., H. Choe, W.M. Kays, and R.J. Moffat, 1976, "Full-Coverage Film Cooling Heat Transfer Study-Summary of Data for Normal-Hole Injection and 30deg
Slant-Hole Injection". Contractor Report CR-2648, NASA.

[5] Andrews, G. E., Alikhanizadeh, M., Asere, A., Hussain, C. I., Koshkbar Azari, M. S. and Mkpadi, M. C., "Small Diameter Film Cooling Holes: Wall Convective Heat Transfer," ASME Paper 86-GT-225 also in Journal of Turbomachinery, Vol. 108, pp.283-289, 1986., 1986.

[6] Andrews, G. E., Alikhanizadeh, M., Bazdidi Tehrani, F., Hussain, C. I. and Khoskbar Azari, M. S., "Small diameter film cooling holes: the influence of hole size and pitch," ASME Paper 87-HT-28, 1987..

[7] Andrews,G.E. and Bazdidi-Tehrani, "Small Diameter Film Cooling Hole Heat Transfer: The Influence of the Number Of Holes," ASME Paper 89-GT-7, 1989.

[8] Andrews, G. E., Bazdidi-Tehrani, F., Hussain, C. I. and Pearson, J. P., "Small Diameter Film Cooling Hole Heat Transfer: The Influence of the Hole Length," ASME Paper 91-GT-344, 1991.

[9] Esgar, J. B., "Turbine Cooling — its Limitations and its Future," AGARD-CP-73- 71, High Temperature Turbines, Paper 14, 1971.

[10] Andrews, G.E. and Mkpadi, M.C. Full coverage discrete hole wall cooling - discharge coefficients. I ASME 83-GT-192, Transactions of the ASME, Journal of Engineering for Power, Vol.106, pp.183-192 (1984).

[11] Bazdidi-Tehrani, F. and Andrews, G. E., "Full Coverage Discrete Hole Film Cooling Investigations of The Effect of Variable Density Ratio (Part II)," ASME Paper 97-GT¬341, 1997.

[12] Kasagi, N., Hirata, M. and Kumada, M. "Studies of full coverage film cooling Part 1: Cooling effectiveness of thermally conductive wall", ASME Paper 81-GT-37, 1981.

[13] Andrews, G. E., Asere, A. A., Gupta, M. L. and Mkpadi, M. C., "Effusion cooling: the influence of the number of holes," ARCHIVE: Proceedings of the Institution of Mechanical Engineers, Part A: Journal of Power and Energy 1990-1996 (vols 204-210), vol. 204, pp. 175-182, 1990.

[14] Andrews, G.E. and Mkpadi, M.C. Full coverage discrete hole wall cooling - discharge coefficients. I ASME 83-GT-192, Transactions of the ASME, Journal of Engineering for Power, Vol.106, pp.183-192 (1984).

[15] Bazdidi-Tehrani, F. and Andrews, G. E., "Full
Coverage Discrete Hole Film Cooling Investigations of The Effect of Variable Density Ratio (Part II)," ASME Paper 97-GT¬341, 1997.

[16] Andrews, G. E., Asere, A. A., Gupta, M. X.,

Mkpadi, M. C. and A., T., "Full Coverage Discrete Hole Film Cooling: The Influence of the Number of Holes and Pressure Loss," ASME Paper 90-GT-61. , 1990.

[17] Andrews, G. E., Alikhanizadeh, M., Bazdidi
Tehrani, F., Hussain, C. I. and Koshkbar Azari, M. S., "Small Diameter Film Cooling Holes: The Influence of Hole Size and Pitch," International Journal of Turbo and Jet Engines, vol. Vol. 5, pp. pp. 61-73, 198

[18] Yavuzkurt, S., Moffat, R. J. and Kays, W. M., 1980, "Full-coverage film cooling. Part 1. Three-dimensional measurements of turbulence structure," Journal of Fluid Mech., vol. 101, Part 1, pp. 129-158. .

[19] Scrittore, J. J., Thole, K. A. and Burd, S. W., 2007, "Investigation of Velocity Profiles for Effusion Cooling of a Combustor Liner," Journal of Turbomachinery, vol. 129, pp. 518-526.

[20] Harrington, M. K., McWaters, M. A., Bogard, D. G., Lemmon, C. A. and Thole, K. A., 2001, "Full-Coverage Film Cooling With Short Normal Injection Holes," Journal of Turbomachinery, vol. 123, pp. 798-805.

[21] Andrews, G. E., Gupta, M. L. and Mkpadi, M. C., 1984, "Combined Radiative and Convective Heat Transfer in an Enclosure," presented at the First UK National Heat Transfer Conference, IChemE Symposium Series No. 86.

[22] Andrews, G. E., Khalifa, I. M., Asere, A. A. and Bazdidi-Tehrani, F., 1995, "Full Coverage Effusion Film Cooling with Inclined Holes," Proc.ASME International Gas Turbine & Aeroengine Congress & Exposition, ASME Paper 95-GT-274.

[23] Bazdidi-Tehrani, F. and Andrews, G. E., 1997, "Full Coverage Discrete Hole Film Cooling Investigations of The Effect of Variable Density Ratio (Part II)," ASME Paper 97-GT-341.

[24] Facchini, B., Tarchi, L., Maiuolo, F. and Coutandin, D., 2011,"Experimental Investigation On The Effects Of A Large Recirculating Area On The Performance Of An Effusion Cooled Combustor Liner," in ASME Conference Proceedings, GT2011-46458.

[25] Jeromin, A., Eichler, C., Noll, B. and Aigner, M., 2008, "Full 3D Conjugate Heat Transfer Simulation and Heat Coefficient Prediction For The Effusion-Cooled Wall of a Gas Turbine Combustor," ASME GT2008-50422.

[26] Kusterer, K., Hagedorn, T., Bohn, D., Sugimoto, T. and Tanaka, R., 2006,"Improvement of a Film-Cooled Blade by Application of the Conjugate Calculation Technique," Journal of Turbomachinery, vol. 128, pp. 572-578.

[27] Silieti, M. Kassab, A. J. and Divo, E., 2009, "Film cooling effectiveness: Comparison of adiabatic and conjugate heat transfer CFD models," International Journal of Thermal
Sciences, vol. 48, pp. 2237-2248.

[28] Bohn, D., Ren, J. and Kusterer, K., 2003,"Conjugate Heat Transfer Analysis for Film Cooling Configurations with Different Hole Geometries," in ASME Conference Proceedings GT2003-38369.

[29] Pedersen, D. R., Eckert, E. R. G. and Goldstein, R. J., 1977, "Film Cooling With Large Density Differences Between the Mainstream and the Secondary Fluid Measured by

the Heat-Mass Transfer Analogy," Journal of Heat Transfer, vol. 99, pp. 620-627.

[30] Sederberg TW, Parry SR. Free-form deformation of solid geometric models. In: David C Evans, Russell J Athay, editors. The proceedings of the 13th annual conference on computer graphics and interactive techniques (SIGGRAPH '86). ACM, New York, NY, USA; 1986. p. 151–60.

[31] Masud A, Bhanabhagvanwala M, Khurram RA. An adaptive mesh rezoning scheme for moving boundary flows and fluid-structure interaction. Comput Fluid 2007;36(1):77–91.

[32] de Boer A, van der Schoot MS, Bijl H. Mesh deformation based on radial basis function interpolation. Comput Struct 2007;85(11–14):784–95.

[33] Jakobsson S, Amoignon O. Mesh deformation using radial basis functions for gradient based aerodynamic shape optimization. Comput Fluid 2007;36(6):1119–36.

[34] Biancolini ME, Biancolini C, Costa E, Gattamelata D, Valentini PP. Industrial application of the meshless morpher RBF morph to a motorbike windshield optimisation. In: The proceedings of the European automotive simulation conference (EASC). Munich. Germany; 2009.

[35] Biancolini ME. Mesh morphing and smoothing by means of radial basis functions (RBF): a practical example using fluent and RBF morph. Handbook of research on computational science and engineering: theory and practice. IGI Global. ISBN13: 9781613501160; 2012.

[36] Caridi D, Wade A. Higher-speed CFD. Professional motorsport magazine; 2012. p. 56. <www.pmw-magazine.com>.

[37] Cella U, Biancolini M. Aeroelastic analysis of aircraft wind-tunnel model coupling structural and fluid dynamic codes. J Aircraft 2012;49(2):407–14.

[38] Khondge A, Sovani S. An accurate, extensive, and rapid method for aerodynamics optimization: the 50:50:50 method. SAE Technical Paper, 2012-01-0174; 2012. doi: http://dx.doi.org/10.4271/2012-01-0174.

[39] M.E. Biancolini et al. Sails trim optimisation using CFD and RBF mesh morphing. Computers & Fluids 93 (2014) 46–60.

[40] Oguntade, H. I., Andrews, G. E., Burns, A., Ingham, D. and Pourkashanian, M., 2011 "Predictions of Effusion Cooling with Conjugate Heat Transfer," in Proceeding of the ASME IGTI Turbo Expo 2011, ASME Paper GT2011-45517, Vancouver, 2011.

[41] Oguntade, H.I., Andrews, G.E., Burns, A.D., Ingham, D.B. and Pourkashanian, M. 2011. " Improved Trench Film Cooling With Shaped Trench Outlets". Proc. ASME Turbo Expo 2011. ASME GT-2011-45253. Also in J. Turbomachinery, 2012.

[42] Oguntade, H.I., Andrews, G.E., Ingham, D.B., Burns, A.D. and Pourkashanian, M., 2012. "Conjugate Heat Transfer Predictions of Effusion Cooling: The Influence of the Coolant Jet Flow Direction on the Cooling Effectiveness". Proc. ASME Turbo Expo 2012, Copenhagen. ASME Paper GT2012-68517.

[43] Oguntade, H.I., Andrews, G.E., Ingham, D.B., Burns, A.D. and Pourkashanian, M., 2012. "Conjugate Heat Transfer Predictions of Effusion Cooling: The Influence of the Injection Hole Size on Cooling Performance". Proc. ASME Turbo Expo 2012, Copenhagen. ASME Paper GT2012-68516.

[44] Oguntade, H.I., Andrews, G.E., Burns, A.D., Ingham, D.B. and Pourkashanian, M., "Conjugate Heat Transfer Predictions of Effusion Cooling with Shaped Trench Outlet". 2014. Proc. ASME Turbo Expo, GT 2014, Dusseldorf, Germany. ASME GT2014-25257.